

A search for VHE counterparts of Galactic *Fermi* bright sources and GeV to TeV spectral characterization

P.H.T. Tam¹, S.J. Wagner¹, O. Tibolla², and R.C.G. Chaves²

¹ Landessternwarte, Universität Heidelberg, Königstuhl, D 69117 Heidelberg, Germany
e-mail: phtam@lsw.uni-heidelberg.de

² Max-Planck-Institut für Kernphysik, P.O. Box 103980, D 69029 Heidelberg, Germany

Preprint online version: May 27, 2019

ABSTRACT

Very high-energy (VHE; $E > 100$ GeV) gamma-rays have been detected from a wide range of astronomical objects, such as SNRs, pulsars and pulsar wind nebulae, active galactic nuclei, gamma-ray binaries, molecular clouds, and possibly star-forming regions as well. At lower energies, sources detected using the Large Area Telescope (LAT) aboard *Fermi* provide a rich set of data which can be used to study the behaviour of cosmic accelerators in the GeV to TeV energy bands. In particular, the improved angular resolution in both bands compared to previous instruments significantly reduces source confusion and facilitates the identification of associated counterparts at lower energies. In this paper, a comprehensive search for VHE gamma-ray sources which are spatially coincident with Galactic *Fermi*/LAT bright sources is performed, and the available GeV to TeV spectra of coincident sources are compared. It is found that bright LAT GeV sources are correlated to TeV sources, in contrast to previous studies using EGRET data. Moreover, a single spectral component seems unable to describe the MeV to TeV spectra of some coincident GeV/TeV sources. It is suggested that gamma-ray pulsars are accompanied by VHE gamma-ray emitting nebulae, a notion that can be tested by VHE observations of these pulsars.

Key words. Gamma rays: observations – Galaxy: general – (Stars) pulsars: general – ISM: supernova remnants – X-rays: binaries

1. Introduction

The knowledge of the very high-energy (VHE; $E > 100$ GeV) sky has greatly improved during the last few years, thanks to the high sensitivity of current imaging atmospheric Cherenkov telescopes (IACTs), e.g. H.E.S.S., MAGIC, and VERITAS. The angular resolution of IACTs is typically $\sim 6'$. The spectra of many objects can be measured from ~ 100 GeV up to several tens of TeV. VHE γ -ray sources now include pulsar wind nebulae (PWN), shell type supernova remnants (SNR), giant molecular clouds, γ -ray binaries, the Galactic Centre, star-forming regions, and active galactic nuclei (AGN). See Aharonian et al. (2008e) for the status of the field in 2008, with progressive updates of new sources in Chaves et al. (2009a,b). However, many of the sources are not yet identified in other wavelengths, e.g., nearly a third of the H.E.S.S. Galactic sources have no firm identification; in many cases, there are multiple low-energy counterparts while, in other cases, no viable counterparts have yet been identified.

Gamma-ray observations of Galactic sources can help us to solve a number of important astrophysical questions, including (1) the physics of pulsars, PWN and SNR; and (2) the origin of cosmic rays. Our galaxy contains a large number of cosmic accelerators, where particles are accelerated to highly-relativistic energies (up to at least 10^{14} eV). The origin of cosmic rays is still not well known, largely because of the lack of directional information of these particles. These very energetic particles can be traced within our Galaxy by a combination of non-thermal X-ray emission and gamma-ray emission via leptonic (like Inverse Compton scattering of electrons, Bremsstrahlung and synchrotron radiation) or hadronic (via the decay of charged and neutral pions, due to interactions of energetic hadrons) processes. Therefore, observations of γ -rays at energies ≥ 100 MeV can probe the sources of particle acceleration.

The Large Area Telescope (LAT), onboard the *Fermi Gamma-ray Space Telescope*, provides the most fruitful information of the non-thermal sky in the energy range from 20 MeV to 300 GeV. The point-source sensitivity of LAT is $\sim 10^{-8}$ ph cm⁻² s⁻¹ above 100 MeV in one year of survey-mode observations (Atwood et al., 2009), which

is an order of magnitude better than that of its predecessor, Energetic Gamma Ray Experiment Telescope (EGRET). Its angular resolution is $\lesssim 0.6^\circ$ above 1 GeV, which is particularly important in identifying γ -ray sources with lower-energy counterparts and revealing their nature (Atwood et al., 2009). As an important step to the first source catalogue, the LAT collaboration has published a bright source list that includes 205 sources using data taken during the first three months of observations (Abdo et al., 2009a). Among them, 121 sources are identified with an AGN and one with the Large Magellanic Cloud, most of the remaining 83 sources are believed to be originated in our own Galaxy. It is natural to see which of them have also been detected at energies ≥ 100 GeV.

Looking for VHE counterpart of LAT sources has at least the following three significance:

1. it helps to identify the nature of the LAT sources through their VHE counterparts;
2. for pulsars, it helps to identify their VHE-emitting nebulae;
3. it provides us with the more complete picture of the γ -ray spectra, thereby better constraining the emission mechanisms (e.g. distinguish between hadronic and leptonic scenarios).

Funk et al. (2008) compare γ -ray sources in the third EGRET catalogue (Hartman et al., 1999) and those 22 then-published H.E.S.S. sources within the region of $l = -30^\circ$ to 30° , $b = -3^\circ$ to 3° (Aharonian et al., 2006f). They do not find spatial correlation between the two populations. Though some coincidence cases are found, the authors conclude that these few cases can be explained by chance coincidence. However, due to the capabilities of the EGRET experiment, this study suffers from the following limitations: (1) The sensitivity of EGRET is lower than that of LAT. The lack of photon statistics leads to poor-constrained spectral index and the spectra end $\lesssim 10$ GeV at the upper end for a typical source; (2) EGRET sources are only localized to degree-scales, which is much larger than the angular resolution of IACTs. The second point is the instrumental reason to explain the weak correlation of EGRET and H.E.S.S. sources (Funk et al.,

2008). These shortcomings are now largely improved by the better performance of LAT over EGRET. In addition to the above caveats mainly related to EGRET capabilities, they do not consider the extension of the VHE sources in their analysis. As such, the full potential of this search is degraded for very extended sources like the supernova RX J1713.7–3946, as pointed out by Tibolla et al. (2009a). After the launch of LAT, one largely benefits from the increased LAT angular resolution over previous studies. As noted in Atwood et al. (2009), EGRET cannot distinguish the GeV emission of SNR RX J1713.7–3946 from 3EG J1714–3857, while the capabilities of LAT allow one to study individual sources in this region, which contain three VHE sources (See Fig. 1 in Aharonian et al., 2008b).

A MILAGRO search of γ -rays from Galactic LAT bright sources has been performed by Abdo et al. (2009g). They found that 14 sources (of the selected 34) show evidence of multi-TeV γ -ray at a significance of $\geq 3\sigma$, although most of the multi-TeV γ -ray emission cannot be established as firm detection on an individual basis (Abdo et al., 2009g).

In this work, VHE counterparts detected using IACTs of each source listed in Abdo et al. (2009a) are searched for, based on spatial coincidence. The extensions of the VHE sources are taken into account and the search is not limited to the H.E.S.S. Galactic plane survey region. Those LAT sources identified with an AGN or the Large Magellanic Cloud are excluded. In the next step, the GeV and TeV parts of the spectra of coincident sources are studied.

2. Search of spatial coincidence

2.1. The *Fermi* and VHE catalogues

Abdo et al. (2009a) present 205 point-like sources with $> 10\sigma$ significance level in the 0.2 – 100 GeV band, based on three months of observations (August 4, 2008 – October 30, 2008). The list is not flux-limited and thus is not uniform. For each source, its position, radius of 95% confidence region, significance of detection, flux in two energy bands (100 MeV–1 GeV and 1–100 GeV), and variability flag. In addition, Abdo et al. (2009a) assign for each source its source class, as well as γ -ray and lower energy association (if any). Those sources that are classified as extragalactic (all AGN and the Large Magellanic Cloud) are not considered in this work.

The remaining source list contains 83 sources, that consists of 15 radio/X-ray pulsars, 15 new pulsars discovered using LAT, 2 high-mass X-ray binaries (HMXBs), one globular cluster (47 Tuc), 13 SNR/PWN candidates¹, and 37 sources without obvious counterparts at lower energy bands (among them the Galactic Centre; Abdo et al., 2009a). Therefore most of the LAT bright sources studied in this work are of Galactic origin. Abdo et al. (2009h) presents the first LAT pulsar catalog. Those 16 pulsars that are not present in the above bright source list are also included in this study.

The number of VHE γ -ray sources is larger than 50 (Aharonian et al., 2008e; Chaves et al., 2009a,b). The VHE γ -ray source positions and source extension in this work are taken from the corresponding publications. At higher energies, the Milagro collaboration reported evidence of multi-TeV emission from several LAT source positions (Abdo et al., 2009g). Only those source candidates with significance larger than 5 are regarded as TeV sources here and are included in this study². With several tens of known sources in both the GeV and TeV bands, a systematic cross-correlation study is conducted.

2.2. Level of spatial coincidence

To quantify the level of spatial coincidence, the following scheme is employed. Let d be the distance between a LAT best-fit centroid position and a nearby VHE source centroid position. The radius of 95%

¹ possibly associated with SNR or PWN, but the emission may come from unknown pulsars

² For example, HESS J1833-105 (Djannati-Atai et al., 2008b), having a significance of 4.0σ only but included in (Abdo et al., 2009h) as a counterpart of LAT pulsar PSR J1833-1034, is not considered here

confidence region for the LAT source is the uncertainty on the centroid position of the given LAT source, which is typically $\sim 0'.1$. Most VHE sources are extended, with a typical extension of $0'.1 - 0'.5$. Let e be the sum of the radius of 95% confidence region and the source extension of the VHE source.

For each LAT source, if a VHE source was found where $d - e < 0$, the source pair is called a spatial coincidence case (i.e. category $Y - \text{Yes}$). Given a possible extended nature of many LAT bright sources, so that the sources seen by LAT and VHE instrument may actually overlap with each other, a category P (for Possible) is defined for pairs where $0 < d - e < 0.3^\circ$; they are slightly offset cases. If no reported VHE source was found with $d - e < 0.3^\circ$: the LAT source falls into the coincidence level N (for No), i.e., no coincidence with any VHE source. If there are several nearby VHE sources, only the closest VHE source would be considered.

2.3. Spatial coincidence GeV/TeV pairs

In the search, 25 coincident cases (Y , among them three are coincident with Milagro source only) and 5 possibly-coincident cases (P) are found. The results are presented in Tables 1, 2, and 3. No reported VHE sources are found in the remaining 69 sources.

According to the nature of the LAT sources, the results are summarized as follows:

1. Eight LAT pulsars are spatially coincident with a source detected using IACTs, which may be the VHE-emitting PWN. In addition, three other have a MILAGRO counterpart, and have not been detected by any IACTs yet.
2. Among the 13 SNR/PWN candidates in the *Fermi* bright source list, more than a half (7) are spatially-coincident with a VHE source, and additionally one being a slightly offset case. The seemingly high fraction of coincidence is partly due to a better coverage of the inner Galaxy region, where most SNR/PWN candidates are located. This results in a generally better sensitivity of this class of sources than other classes.
3. The two high-mass X-ray binaries listed in BSL (0FGL J0240.3+6113/LS I +61 303 and 0FGL J1826.3–1451/LS 5039) are both found spatially coincident with a VHE gamma-ray source, identified with the same corresponding binary.
4. Five out of the 37 unidentified 0FGL sources are spatially coincident with a VHE gamma-ray source. The number increases to nine if possible coincidence cases are included.

With such a large number of coincident cases, the relation of the GeV and TeV sources are explored. In the next section, the gamma-ray spectral energy distributions are constructed for those coincident and possibly coincident GeV/TeV source pairs with published VHE spectrum.

3. The gamma-ray spectral energy distributions

3.1. Construction of power law spectrum in the LAT range

In Abdo et al. (2009a) are given photon fluxes and their errors in two energy bands: low energy (100 MeV–1 GeV) and high energy (1 – 100 GeV). Since photon spectra are not given in the bright source list, we attempt to estimate the spectra of individual sources.

Assuming a single power law, F_{23} and F_{35} (photon flux in the low energy ($10^2 - 10^3$ MeV) and high energy ($10^3 - 10^5$ MeV) band, respectively) are given by $F_{23} = k \int_{0.1}^1 E^{-\Gamma} dE$ and $F_{35} = k \int_1^{100} E^{-\Gamma} dE$, where E is measured in GeV, Γ is the photon index, and k is the normalization at 1 GeV. From these two expressions, k and Γ can be obtained. Using the available flux errors (ΔF_{23} , ΔF_{35}), uncertainties in k and Γ (Δk and $\Delta \Gamma$) are obtained by error propagation. The spectra in form of “bowties” are then constructed. For those for which F_{23} is given as a $2 - \sigma$ upper limit, the calculated Γ can be treated as an upper limit and the reconstructed spectra can be seen as the “softest possible” power-law spectra. The power-law spectra are drawn from 100 MeV up to a certain maximum energy, E_{\max} (≤ 100 GeV), which is defined by requiring

that the photon spectrum above E_{\max} contains 10 photons over the three months of observations³. E_{\max} ranges from ~ 3 GeV to 100 GeV. The single power law assumption does not hold in general. Given the limited information available in the bright source list, such an assumption should be seen as a very rough estimation of the source spectra and it is used in this work for a visual GeV/TeV spectral comparison. A cut-off between the GeV and TeV bands has been measured for several sources including pulsars. Therefore, we also plot the best fit spectra, when a detailed spectrum seen with LAT is available in the literature (Vela, Crab, Geminga, PSR J1706–44, and LS I +61 303). For the cases of 0FGL J0617.4+2234 and 0FGL J1746.0–2900, the double power-law spectra derived for 3EG J0617+2238 and 3EG J1746–2851, respectively, by Bertsch et al. (2000) are also shown for comparison.

3.2. The MeV–TeV SEDs

The sources concerned here are those 0FGL/VHE pairs with spatial coincidence levels Y and P and with available VHE spectral information in the literature. In the case of HESS J1923+141 where only a VHE flux is given, a spectral index is assumed for plotting purposes. In addition, there are three pulsars for which a MILAGRO candidate counterpart is reported but without VHE detection (see Table 2).

Spectral energy distributions (SEDs) in the energy range from 100 MeV to >1 TeV of the 26 cases are depicted in Fig. 1 to 9. Systematic errors in spectral indices and normalization are not shown, which for TeV spectra are $\sim 20\%$ for most sources and for GeV spectra are $\sim 20\text{--}30\%$ (the latter is inferred from flux estimation systematics in Abdo et al., 2009a). An overall inspection of the SEDs immediately tells that single power laws all the way from 200 MeV to ~ 10 TeV cannot describe most GeV–TeV gamma-ray spectra. This is not surprising given the large range in photon energy span (i.e. five orders of magnitude), as no emission mechanism is expected to be unbroken for such a large energy span. The only example for which an unbroken power law may still work is 0FGL J1836.1–0727/HESS J1837–069, which is a possible coincident pair (P). The most common board-band behaviors are a cut-off at energies below ~ 100 GeV (dominating in the PSR class), as well as a spectral break between the LAT and the VHE bands (dominating in the unidentified LAT sources).

The SEDs of the LAT source classes including pulsars, SNR/PWN candidates, and unidentified γ -ray sources are presented in this section. LS I +61 303 and the Galactic centre region are discussed in Sect. 4.5 and 4.6, respectively.

3.2.1. Pulsars

Figure 1 shows the four gamma-ray pulsars known in the EGRET era, Fig. 2 shows the three radio pulsars first detected in gamma-rays by LAT, and Fig. 3 shows the three new pulsars discovered in a blind pulsation search in the LAT data (Abdo et al., 2009b). Besides the Crab, no off-pulse emission is found in the LAT data of other 8 pulsars, suggesting that most emission seen with LAT is pulsed emission and originates from the pulsars. On the other hand, extended regions are seen at energies above 100 GeV in these 8 cases (except for the Crab, which appears point-like to all IACTs). The very high-energy emission (>100 GeV) is unpulsed and many of them (e.g. Vela X) have been attributed to pulsar wind nebulae, although in some cases there exist other possibilities to explain the VHE source.

The SEDs of the class pulsars essentially depict the pulsed component at the LAT energy band and the unpulsed component at the VHE band. It is clear that the emission below and above ~ 100 GeV comes from two different emission regions, e.g. pulsed emission from pulsar magnetosphere and unpulsed emission from pulsar wind nebula. It can be seen that (1) a cut-off must exist between the LAT “bowties” and the corresponding VHE spectra (with the notable exception of the Crab) – this is demonstrated with detailed spectral study of pulsars (e.g., Abdo et al., 2009h); (2) the energy output at GeV energies is at least an

order of magnitude higher than that in the VHE band. This indicates that for the pulsar population presented in this section, the pulsar wind nebulae radiate less energy than the gamma-ray pulse emitting regions.

However, the power-law derived LAT spectra (the “bowtie”) are no good representations of the reported spectra for individual sources. It is demonstrated in Fig. 1 where both “bowtie” spectra and the derived spectra in Abdo et al. (2009h) are shown. In all the other cases, only the spectra as presented in Abdo et al. (2009h) are depicted.

3.2.2. SNR/PWN candidates

The SEDs of those 0FGL sources classified as SNR/PWN candidates are shown in Fig. 4 and Fig. 5. The GeV–TeV spectral connection varies among the sources in this class. The TeV spectra are not simply the tails of the GeV spectra. There are cases where the extrapolation of the LAT “bowtie” to TeV energies is at least an order of magnitude higher than the measured VHE flux level (e.g. the position-overlapped case 0FGL J1801.6–2327/HESS J1801–233, a cut-off is induced between the two energy bands), while for another overlapped case (0FGL J1834.4–0841/HESS J1834–087) the “bowtie”-extrapolation to VHE band is below the measured VHE level and a second spectral component above ~ 200 GeV is needed to explain the TeV excess.

There are by far only one indication (of 0FGL J0617.4+2234) that a broken power law describe the LAT spectrum better than a single power law does. The “bowties”, which are derived *a priori* from power laws, may be closer to the real spectra compared to the case of pulsars. If that is the case for 0FGL J1801.6–2327/HESS J1801–233 and 0FGL J1923.0+1411/HESS J1923+141, a spectral break may occur at energies at the largely unexplored energy range of 10–100 GeV for these two sources⁴.

3.2.3. Unidentified LAT sources

The SEDs of those 0FGL sources without obvious counterparts are shown in Fig. 6 and Fig. 7. There is by far no published spectra of this LAT source class which suggests that a broken power law describes the LAT spectrum better than a single power law does. For the case of 0FGL J1839.0–0549/HESS J1841–055, the spectrum may span from ~ 100 MeV to ~ 80 TeV, with a possible break within or close to the “energy gap” at $\sim 60\text{--}500$ GeV. The detection of a LAT source associated with HESS J1841–055 is said to likely in Tibolla et al. (2009a) based on the VHE luminosity of the H.E.S.S. source. If the GeV and TeV sources are indeed associated, they represent a group of “dark accelerators” which have a board gamma-ray spectrum.

All SEDs are consistent with the notion that a spectral break exists between the two energy bands, except for the case of 0FGL J1805.3–2138/HESS J1804–216, a spatial-coincident case (Y).

3.3. Flux and photon index comparison in the GeV and TeV energy bands

A comparison of the flux levels in the GeV and TeV energy bands for coincident GeV/TeV sources (category Y) is depicted. Figure 10 shows the photon flux in the 100 MeV – 1 GeV band plotted against that in the 1–10 TeV band. For most sources, photon flux in the 1–10 TeV band, $F_{1-10\text{TeV}}$, is about 10^{-5} to 10^{-6} that in the 0.1–1 GeV band. Figure 11 shows the photon flux in the 1–100 GeV band plotted against that in the 1–10 TeV band. For most sources, photon flux in the 1–10 TeV band, $F_{1-10\text{TeV}}$, is about 10^{-4} to 10^{-5} that in the 1–100 GeV band. Figure 12 depicts the photon index in the 0.1–100 GeV band derived according to Sect. 3.1 against photon index in the 1–10 TeV band. It can be seen that the TeV spectra are similar or a bit harder compared to the GeV spectra for most sources, i.e. $\Gamma_{1-10\text{TeV}} - \Gamma_{0.1-100\text{GeV}} \sim 0 - 1$.

³ Using the LAT on-axis effective area above 1 GeV of ~ 8000 cm² and a mean on-axis exposure of ~ 1 Ms (Abdo et al., 2009a)

⁴ The LAT spectrum for 0FGL J1801.6–2327 is the softest possible power law, while the HESS J1923+141 spectrum is derived assuming a power law index of $\Gamma = 2.8$.

4. Notes on selected sources

Although detailed analysis of the LAT data for each individual source is beyond the scope of this paper, some comments on the following sources are given.

4.1. Crab pulsar and nebula

The Crab region is one of the best-studied non-thermal objects on the sky. The pulse emission above 100 MeV and up to ~ 10 GeV is clearly detected with LAT. Two strong peaks are seen in the phase histogram. A fit using a power law with exponential cut-off of the pulsed emission gives a cut-off energy of ~ 8.8 GeV (Grondin et al., 2009). There is evidence of pulse emission up to ~ 25 GeV, as measured using the MAGIC telescope (Aliu et al., 2008). The reported flux level by MAGIC is consistent with the cut-off functional form of the LAT spectrum mentioned above.

An unpulsed component was already evidenced in the EGRET data (de Jager et al., 1996). The LAT measurement of this component can be well fit by a single power law with $\Gamma \sim 1.9$ up to ~ 300 GeV. This unpulsed spectrum is naturally joined with the VHE spectra measured by Cherenkov arrays such as MAGIC, H.E.S.S. and VERITAS (Grondin et al., 2009). In particular, there appears to be a *turn-over* in the MAGIC spectrum below ~ 100 GeV (Albert et al., 2008).

4.2. Vela pulsar and Vela X

The Vela pulsar is the strongest persistent GeV source and the first target of LAT observations. The complex pulse profile is dominated by two peaks with a pronounced “bridge” between them. The phase-averaged spectrum, which is essentially the pulse emission, can be well described by a power law with exponential cut-off at energy ~ 2.9 GeV. Off-pulse emission is much weaker, and a 95% CL upper limit photon flux of $1.8 \times 10^{-7} \text{ cm}^{-2} \text{ s}^{-1}$ is derived at the pulsar position in the 0.1–10 GeV band (shown in Fig. 1, Abdo et al., 2009c).

To the south of the pulsar, an extended VHE source spatially coincident with the Vela X region, HESS J0835–455, has been detected. The observations represent the first measurement of a SED peak in a VHE source (Aharonian et al., 2006b). The power law with exponential cut-off fit of this pulsar wind nebula is reproduced in Fig. 1. An analysis of the Vela X region does not establish a nebula component based on the first three months of LAT observations (Lemoine-Goumard et al., 2009).

4.3. Geminga

The Geminga pulsar is the first known radio-quiet gamma-ray pulsar in the sky. While EGRET data are well fit by a single power law up to 2 GeV (but show evidence of cut-off above 2 GeV, Mayer-Hasselwander et al., 1994), the cut-off energy is determined to be ~ 2.6 GeV using the first seven months of LAT data (Celik et al., 2009). There is a seemingly excess at ~ 20 GeV as compared to the power law with exponential cut-off fit. The reason may be due to low statistics or analysis chain, but it is possible that a separate component arises from here (Celik et al., 2009). There is as yet no evidence for an unpulsed emission.

Evidence of multi-TeV emission around the pulsar is reported in the MILAGRO survey of Galactic plane (Abdo et al., 2007) and the search of MILAGRO counterpart of *Fermi* sources (Abdo et al., 2009g), using point source analysis, at $\sim 3\sigma$ (post-trial) significance levels. Assuming extended emission, the significance increases to 6.3σ at the position of the pulsar. If the detection is true, the extension of the MILAGRO emission is ~ 2.6 . At a distance of only ~ 250 pc, this extent is similar to more distant PWN (Abdo et al., 2009g). On the other hand, VERITAS observations result in no detection, but a 99% CL flux upper limit (above 300 GeV) of $2 \times 10^{-12} \text{ cm}^{-2} \text{ s}^{-1}$, assuming a point source emission from the pulsar (Finnegan et al., 2009). Although with reduced sensitivity of very extended source (which scales as θ^{-1} with θ being the extension),

observations of IACTs on Geminga are crucial to verify the MILAGRO claim, thus help to understand the gamma-ray emission from Geminga.

4.4. PSR B1706–44

Gamma-ray pulsations from PSR B1706–44 were discovered by EGRET; the observations revealed a triple-peaked pulse profile but no evidence for unpulsed emission (Thompson et al., 1996). More recently, the pulsar was also detected by *Fermi*/LAT as the bright source 0FGL J1709.7–4428. The phase-averaged spectra measured by EGRET and LAT are both well-described by a broken power law (up to 30 GeV, in the case of the LAT spectrum). The break energy measured by LAT is 3 GeV, while in deriving the EGRET spectrum, it is fixed at 1 GeV (Thompson et al., 1996; Bertsch et al., 2000). The LAT power-law index changes from ~ 1.9 (below 3 GeV) to ~ 3.3 (above 3 GeV), as shown in Fig. 1. This spectrum and the power-law spectrum derived using the method described in Sect. 3.1 are both consistent with the photon flux in the 1–100 GeV band reported in Abdo et al. (2009a).

Discovery of an extended source of VHE emission in the vicinity of PSR B1706–44 was recently reported by H.E.S.S. (Hoppe et al., 2009). The TeV source is quite hard ($\Gamma \sim 2$), more so than the high-energy part of the pulsar spectrum. The VHE γ -ray emission is suggested to be related either to a relic PWN of PSR B1706–44 and/or the SNR G343.1–2.3 (Hoppe et al., 2009).

4.5. LS I +61 303

LS I +61 303 is the first X-ray binary where periodic γ -ray emission has been detected in both GeV (Abdo et al., 2009d) and TeV energies (Acciari et al., 2009a; Albert et al., 2009). The “bowtie” looks nicely connected to the measured VHE spectrum, but a cut-off energy at ~ 6 GeV is reported (Abdo et al., 2009d). Furthermore, the timing measurements at GeV and TeV bands show that the maximum emission occurs at different orbital phases, namely, close to periastron for <100 GeV emission and close to apastron for VHE emission. This suggests different emission mechanisms in the two bands, as noted in (Abdo et al., 2009d).

4.6. Galactic Centre Region

The Galactic Center is among the richest and most complex regions in the Galaxy, due to the large number of possible sources and the difficulty to correctly model the diffuse emission due to cosmic-ray interaction with the local molecular clouds complex; hence it deserves an independent treatment. This problem is extremely relevant at GeV energies, as shown by EGRET measurements; hence the discovery of new VHE sources close to the Galactic Center is relevant for the studies of the role of diffuse Galactic emission versus resolved sources in this region (Tibolla et al., 2009a).

One GeV source, 0FGL J1746.0–2900, is detected with a significance of 36σ in the neighbourhood of the Galactic Centre (Abdo et al., 2009a). The best fit position for 0FGL J1746.0–2900 is $l = 359^\circ 59' 16''.1, b = -0^\circ 6' 40''.7$ with a 95% C.L. error radius of $4'$ (Cohen-Tanugi et al., 2009). The H.E.S.S. collaboration also reported a strong detection of a source towards the Galactic Centre, localized at $l = 359^\circ 56' 33''.3 \pm 9''.7, b = -0^\circ 2' 40''.6 \pm 10''$ (Aharonian et al., 2006h), or in a more recent analysis (van Eldik et al., 2008) at $l = 359^\circ 56' 41''.1 \pm 6''.4$ (stat), $b = -0^\circ 2' 39''.2 \pm 5''.9$ (stat). Based on the procedure described in Sect. 2.2, the 0FGL J1746.0–2900/HESS J1745–290 pair falls into the category of slightly-offset cases. With better photon statistics, one of the fundamental questions that the LAT can hopefully address is whether the GeV and TeV sources are indeed spatially inconsistent.

The SED depicting 0FGL J1746.0–2900 and HESS J1745–290 is shown in Fig. 9. The spectra in two bands do not seem to connect naturally, and there seems to be a one order-of-magnitude drop-off in the energy range ~ 10 –100 GeV. Although detailed analysis of the LAT data is out of the scope of this paper, this simple inspection does not support the notion that they are from the same emission component (al-

though large uncertainty in systematics in this region does not allow for any stronger conclusion). For reference, the broken power law fit of 3EG J1746–2851 (Bertsch et al., 2000) is also shown in Fig. 9.

5. Discussion

In this work, the first comparison of the GeV and VHE sources after the launch of LAT is presented, which takes the advantage of the much better LAT angular resolution and sensitivity compared to EGRET.

Below are a list of preliminary results drawn from this work.

1. With the better localization and morphological information of VHE sources over 0FGL sources, the nature of the LAT sources may be better revealed through their VHE counterparts. Table 1 lists the potential counterparts of some VHE sources which are coincident with 0FGL sources. For example, HESS J1804–216 may be related to W 30, which in turn may help to understand the nature of the unidentified source 0FGL J1805.3–2138.
2. First results of several LAT-detected pulsars show cut-offs at energies ~ 1 – 10 GeV, similar to the assessment of Funk et al. (2008) for EGRET pulsar systems. Therefore, a VHE counterpart (~ 0.1 – 10 TeV) of a LAT pulsar most likely represent the associated PWN, with a shell-type supernova being a viable alternative. This is particularly important for those new pulsars discovered by LAT. The VHE counterparts coincident with the three LAT pulsars may be the associated PWN, although other explanations (e.g. shell-type SNR) are also possible. Whether typical gamma-ray pulsars are accompanied by VHE-emitting nebulae can be tested by VHE observations of these pulsars.
3. Through broad-band γ -ray spectra obtained for SNRs, one may in principle distinguish between hadronic and leptonic scenarios. A simulation of SNR RX J1713.7–3946 in 5 years of LAT observations (Atwood et al., 2009) shows that the energy flux level for the hadronic scenario differs by around a factor of two from that for the leptonic scenario, and that a spectral break may be more prominent for the leptonic scenario. The SNR sample shown in Figs. 4 and 5 do not seem to support either scenario, although it is too early to draw any conclusion. If a hadronic scenario is to be found more viable, this would greatly advance the current consensus that shell-type SNRs are cosmic-ray sources.
4. Previous studies did not reveal a strong correlation between the GeV/TeV populations. Reimer et al. (2008) list 16 H.E.S.S. sources without 3EG counterpart. Among them, new associations are found in the present study and are presented in Table 4, thanks mostly to the discovery of new GeV sources with LAT. These authors also present 11 sources in the third EGRET catalogue without H.E.S.S. counterpart. Among them, 0FGL J1709.7–4428 (the 0FGL counterpart of 3EG J1710–4439; Abdo et al., 2009a) is now found associated with HESS J1708–443, a new source reported in Hoppe et al. (2009).
5. All GeV and TeV connecting cases during the EGRET era are essentially consistent with one single spectral component (See Figs. 4, 5 and 6 in Funk et al., 2008). With the much better sensitivity of LAT, new relations between the GeV and TeV spectra are apparent in the SEDs. The SNR candidate 0FGL J1834.4–0841 and the unidentified 0FGL J1805.3–2138 (and their likely VHE counterparts) represent the first examples for which the GeV/TeV spectrum cannot be treated as a single emission component. A similar conclusion made for an XRB (LS I 61 303) is reached by Abdo et al. (2009d), based on the light curves and spectral incompatibility of this source in the two bands.
6. Abdo et al. (2009g) invoke a probability that many unidentified LAT sources are extragalactic, so as to explain the low rate of finding coincident MILAGRO emission among the unidentified LAT sources. This notion can also explain the non-detection of VHE counterparts of a majority of the unidentified LAT sources. On the other hand, the extended nature of all the five spatially coincident cases (HESS J1023–575, HESS J1804–216, HESS J1841–055, HESS J1843–033, HESS J1848–018; if proved to be real association) would exclude an extragalactic origin of the corresponding LAT sources.

7. Although VHE observations only cover a small part of the whole sky, they do cover the majority of the inner Galaxy region, e.g., the H.E.S.S. telescopes have surveyed the region of $l = -85^\circ$ to 60° , $b = -3^\circ$ to 3° (Chaves et al., 2009b). In this region, there are 41 *Fermi* bright sources. Among them, 16 are found coincident with a VHE counterpart. This fraction ($\sim 2/5$) is higher than that for EGRET where about 1/4 of the EGRET sources (in a smaller region) are found to have a coincident VHE counterpart (Funk et al., 2008). Moreover, the number raises to 21 (out of 41) if slightly-offset cases are included and the fraction becomes 50%. The LAT radii of 95% confidence region are mostly much smaller than EGRET error boxes, which further strengthen the case of a higher fraction for LAT. Even though the VHE extension is taken into account in this study (but not in Funk et al., 2008), a typical extension is of the same order as a LAT confidence radius. A breakdown of the number of coincidence cases for each source population in the region of $l = -85^\circ$ to 60° , $b = -3^\circ$ to 3° is shown in Table 5.

6. Conclusion

In this work, we search for possible VHE counterparts detected using IACTs of each source listed in Abdo et al. (2009a), based on spatial coincidence. This study largely benefits from the increased LAT angular resolution and its better sensitivity over previous studies.

Compared to the EGRET era, not only are there more coincident sources (improvement in quantity), improvements in quality start to emerge. With the much better sensitivity of LAT, weaker sources are detected which are unknown in the EGRET era. New relations between the GeV and TeV spectra are revealed. A single spectral component is unable to describe some sources detected in both GeV and TeV energies. Two spectral components may be needed in these cases to accommodate the SEDs, where the VHE flux is higher than a power-law extrapolation from GeV energies.

The high fraction of *Fermi* bright sources spatially coincident with a VHE counterpart cannot be a chance coincidence, in stark contrast with the conclusion in Funk et al. (2008). This means that there exists a common GeV/TeV source population. A notion has emerged that gamma-ray pulsars and their PWN/SNR constitute a significant fraction of the >100 MeV sky.

Acknowledgements. We thank Emma Oña-Wilhelmi and Werner Hofmann for discussion.

References

- Abdo, A. A., Ackermann, M., Ajello, M., et al. (Fermi/LAT Collaboration), 2009a, *ApJS*, 183, 46
- Abdo, A. A., Ackermann, M., Ajello, M., et al. (Fermi/LAT Collaboration), 2009b, *Science*, 325, 840
- Abdo, A. A., Ackermann, M., Atwood, W. B., et al. (Fermi/LAT Collaboration), 2009c, *ApJ*, 696, 1084
- Abdo, A. A., Ackermann, M., Ajello, M., et al. (Fermi/LAT Collaboration), 2009d, *ApJ*, 701, L123
- Abdo, A. A., Ackermann, M., Ajello, M., et al. (Fermi/LAT Collaboration), 2009e, *ApJ*, 706, L1
- Abdo, A. A., Ackermann, M., Ajello, M., et al. (Fermi/LAT Collaboration), 2009f, *ApJ*, 706, L56
- Abdo, A. A., Allen, B. T., Aune, T., et al. (MILAGRO Collaboration), 2009g, *ApJ*, 700, L127
- Abdo, A. A., for the Fermi LAT collaboration, 2009h, submitted, arXiv:0910.1608
- Abdo, A. A., Allen, B., Berley, D., et al. (MILAGRO Collaboration), 2007, *ApJ*, 664, L91
- Acciari, V. A., Aliu, E., Arlen, T., et al. (VERITAS Collaboration) 2009a, *ApJ*, 700, 1034
- Acciari, V. A., Aliu, E., Arlen, T., et al. (VERITAS Collaboration) 2009b, *ApJ*, 698, L133
- Aharonian, F. A., Akhperjanian, A. G., Aye, K.-M., et al. (H.E.S.S. Collaboration) 2005a, *A&A*, 436, L17
- Aharonian, F. A., Akhperjanian, A. G., Beilicke, M., et al. (HEGRA Collaboration) 2005b, *A&A*, 431, 197
- Aharonian, F. A., Akhperjanian, A. G., Bazer-Bachi, A. R., et al. (H.E.S.S. Collaboration) 2006a, *A&A*, 448, L19
- Aharonian, F. A., Akhperjanian, A. G., Bazer-Bachi, A. R., et al. (H.E.S.S. Collaboration) 2006b, *A&A*, 448, L43
- Aharonian, F. A., Akhperjanian, A. G., Bazer-Bachi, A. R., et al. (H.E.S.S. Collaboration) 2006c, *Nature*, 440, 1018
- Aharonian, F. A., Akhperjanian, A. G., Bazer-Bachi, A. R., et al. (H.E.S.S. Collaboration) 2006d, *A&A*, 457, 899
- Aharonian, F. A., Akhperjanian, A. G., Bazer-Bachi, A. R., et al. (H.E.S.S. Collaboration) 2006e, *A&A*, 460, 743
- Aharonian, F. A., Akhperjanian, A. G., Bazer-Bachi, A. R., et al. (H.E.S.S. Collaboration) 2006f, *ApJ*, 636, 777
- Aharonian, F. A., Akhperjanian, A. G., Bazer-Bachi, A. R., et al. (H.E.S.S. Collaboration) 2006g, *A&A*, 456, 245
- Aharonian, F. A., Akhperjanian, A. G., Bazer-Bachi, A. R., et al. (H.E.S.S. Collaboration) 2006h, *Phys. Rev. Lett.*, 97, 221102
- Aharonian, F. A., Akhperjanian, A. G., Bazer-Bachi, A. R., et al. (H.E.S.S. Collaboration) 2007a, *A&A*, 467, 1075
- Aharonian, F. A., Akhperjanian, A. G., Bazer-Bachi, A. R., et al. (H.E.S.S. Collaboration) 2007b, *A&A*, 472, 489
- Aharonian, F. A., Akhperjanian, A. G., Barres de Almeida, U., et al. (H.E.S.S. Collaboration) 2008a, *A&A*, 477, 481
- Aharonian, F. A., Akhperjanian, A. G., Barres de Almeida, U., et al. (H.E.S.S. Collaboration) 2008b, *A&A*, 490, 685
- Aharonian, F. A., Akhperjanian, A. G., Barres de Almeida, U., et al. (H.E.S.S. Collaboration) 2008c, *A&A*, 481, 401
- Aharonian, F. A., Akhperjanian, A. G., Barres de Almeida, U., et al. (H.E.S.S. Collaboration) 2008d, *A&A*, 477, 353
- Aharonian, F., Buckley, J., Kifune, T., & Sinnis, G. 2008e, *Reports on Progress in Physics*, 71, 096901
- Aharonian, F. A., Akhperjanian, A. G., Anton, G., et al. (H.E.S.S. Collaboration) 2009, *A&A*, 499, 723
- Albert, J., Aliu, E., Anderhub, H., et al. (MAGIC Collaboration) 2007, *ApJ*, 664, L87
- Albert, J., Aliu, E., Anderhub, H., et al. (MAGIC Collaboration) 2008, *ApJ*, 674, 1037
- Albert, J., Aliu, E., Anderhub, H., et al. (MAGIC Collaboration) 2009, *ApJ*, 693, 303
- Aliu, E., for the VERITAS Collaboration, 2009, "Search for VHE γ -ray emission in the vicinity of selected pulsars of the Northern Sky with VERITAS", AIP Conference Proceedings, 1085, 324
- Aliu, E., Anderhub, H., Antonelli, L. A., et al. (MAGIC Collaboration) 2008, *Science*, 322, 1221
- Atwood, W. B., Abdo, A. A., Ackermann, M., et al. (Fermi/LAT Collaboration) 2009, *ApJ*, 697, 1071
- Berge, D., Funk, S., & Hinton, J. A. 2007, *A&A*, 466, 1219
- Bertsch, D. L., Hartman, R. C., Hunter, S. D., et al. 2000, *American Institute of Physics Conference Series*, 510, 504
- Celik, O., on behalf of the Fermi-LAT Collaboration, 2009, "Fermi-LAT observations of the Geminga pulsar", to be published in the proceedings of the 31st International Cosmic Ray Conference
- Chaves, R. C. G., Renaud, M., Lemoine-Goumard, M., & Goret, P., for the H.E.S.S. Collaboration, 2009a, AIP Conference Proceedings, 1085, 219
- Chaves, R. C. G., on behalf of the H.E.S.S. Collaboration, 2009b, "Extending the H.E.S.S. Galactic Plane Survey", to be published in the proceedings of the 31st International Cosmic Ray Conference
- Chaves, R. C. G., de Oña Wilhemi, E., & Hoppe, S., for the H.E.S.S. Collaboration, 2009c, AIP Conference Proceedings, 1085, 372
- Cohen-Tanugi, J., Pohl, M., Tibolla, O., Parent, D., Nuss, E. for the Fermi/LAT Collaboration, 2009, to be published in the proceedings of the 31st International Cosmic Ray Conference
- Djannati-Atai, A., de Jager, O. C., Terrier, R., Gallant, Y. A., Hoppe, S., for the H.E.S.S. Collaboration, 2008a, Proceedings of the 30th International Cosmic Ray Conference; Rogelio Caballero, Juan Carlos D'Olivo, Gustavo Medina-Tanco, Lukas Nellen, Federico A. Sánchez, José F. Valdés-Galicia (eds.); Universidad Nacional Autónoma de México, Mexico City, Mexico, 2, 823
- Djannati-Atai, A., Oña-Wilhelmi, E., Renaud, M., Hoppe, S., for the H.E.S.S. Collaboration, 2008b, Proceedings of the 30th International Cosmic Ray Conference; Rogelio Caballero, Juan Carlos D'Olivo, Gustavo Medina-Tanco, Lukas Nellen, Federico A. Sánchez, José F. Valdés-Galicia (eds.); Universidad Nacional Autónoma de México, Mexico City, Mexico, 2, 863
- Dubois, F., Glüick, B., de Jager, O. C., et al. 2009, Proceedings of the 31st ICRC, Łódź, Poland
- van Eldik, C., Bolz, O., Braun, I., Hermann, G., Hinton, J. & Hofmann, W. 2008, Proceedings of the 30th International Cosmic Ray Conference; Rogelio Caballero, Juan Carlos D'Olivo, Gustavo Medina-Tanco, Lukas Nellen, Federico A. Sánchez, José F. Valdés-Galicia (eds.); Universidad Nacional Autónoma de México, Mexico City, Mexico, 2, 589
- Feldman, G. J., & Cousins, R. D. 1998, *Phys. Rev. D.*, 57, 3873
- Fiasson, A., Marandon, V., Chaves, R. C. G., Tibolla, O., for the H.E.S.S. Collaboration, 2009, "Discovery of a VHE gamma-ray source in the W51 region", to be published in the proceedings of the 31st International Cosmic Ray Conference
- Finnegan, G., on behalf of the VERITAS Collaboration, 2009 "Search for TeV emission from Geminga by VERITA", to be published in the proceedings of the 31st International Cosmic Ray Conference
- Funk, S., Hermann, G., Hinton, J. A. et al. 2004, *Astropart. Phys.*, 22, 285
- Funk, S., Reimer, O., Torres, D. F., & Hinton, J. A. 2008, *ApJ*, 679, 1299
- Gargano, F. for the Fermi/LAT Collaboration, 2009, "Spectral analysis of EGRET pulsars", to be published in the proceedings of the 31st International Cosmic Ray Conference
- Grondin, M.-H., on behalf of the Fermi-LAT Collaboration, 2009, "Fermi-LAT observations of the Crab nebula and pulsar", to be published in the proceedings of the 31st International Cosmic Ray Conference
- Halpern, J. P., Camilo, F., Gotthelf, E. V., et al. 2001, *ApJ*, 552, L125
- Hartman, R. C., Bertsch, D. L., Bloom, S. D., et al. 1999, *ApJS*, 123, 79
- Hillas, A. M. 1996, *Space Sci. Rev.*, 75, 17
- Hoppe, S., for the H.E.S.S. Collaboration, 2008, Proceedings of the 30th International Cosmic Ray Conference; Rogelio Caballero, Juan Carlos D'Olivo, Gustavo Medina-Tanco, Lukas Nellen, Federico A. Sánchez, José F. Valdés-Galicia (eds.); Universidad Nacional Autónoma de México, Mexico City, Mexico, 2, 579, preprint[arXiv:0710.3528]
- Hoppe, S., de Oña Wilhemi, E., Khelifi, B., Chaves, R. C. G., de Jager, O. C., Stegmann, C., Terrier, R., for the H.E.S.S. Collaboration, 2009, "Detection of very-high-energy gamma-ray emission from the vicinity of PSR B1706-44 with H.E.S.S.", to be published in the proceedings of the 31st International Cosmic Ray Conference, preprint[arXiv:0906.5574]
- Hinton, J. 2009, *New Journal of Physics*, 11, 055005
- de Jager, O. C., Harding, A. K., Michelson, P. F., Nel, H. I., Nolan, P. L., Sreekumar, P., & Thompson, D. J. 1996, *ApJ*, 457, 253
- Lamb, R. C., & Macomb, D. J. 1997, *ApJ*, 488, 872
- Lemoine-Goumard, M., and Grondin, M.-H., on behalf of the Fermi-LAT Collaboration and the Pulsar Timing Consortium, 2009, "Fermi-LAT observations of the Vela X region", to be published in the proceedings of the 31st International Cosmic Ray Conference
- Li, T.-P., & Ma, Y.-Q. 1983, *ApJ*, 272, 317
- Mayer-Hasselwander, H. A., Bertsch, D. L., Brazier, K. T. S., et al. 1994, *ApJ*, 421, 276
- Ng, C.-Y., Roberts, M. S. E., & Romani, R. W. 2005, *ApJ*, 627, 904
- Ohm, S., Horns, D., de Oña Wilhemi, E., for the H.E.S.S. Collaboration, 2009, "H.E.S.S. observations towards the massive stellar cluster Westerlund 1", to be published in the proceedings of the 31st International Cosmic Ray Conference
- Reimer, O., Funk, S., Torres, D. F., & Hinton, J. 2008, Proceedings of the 30th International Cosmic Ray Conference; Rogelio Caballero, Juan Carlos D'Olivo, Gustavo Medina-Tanco, Lukas Nellen, Federico A. Sánchez, José F. Valdés-Galicia (eds.); Universidad Nacional Autónoma de México, Mexico City, Mexico, 2, 613

- de los Reyes, R., Bednarek, W., Camara, M., & M. Lopez for the MAGIC Collaboration, 2009, "Upper limits for pulsars with MAGIC (2005/2006 observations)", to be published in the proceedings of the 31st International Cosmic Ray Conference
- Thompson, D. J., Bailes, M., Bertsch, D. L., et al. 1996, *ApJ*, 465, 385
- Tibolla, O., on behalf of the H.E.S.S. Collaboration, 2009a, AIP Conference Proceedings, 1112, 211
- Tibolla, O., Komin, N., Kosack, K., & Naumann-Godo, M., on behalf of the H.E.S.S. Collaboration, 2009b, "A new source discovered close to the Galactic Center: HESS J1741-302", AIP Conference Proceedings, 1085, 249
- Zepka, A., Cordes, J. M., Wasserman, I., & Lundgren, S. C. 1996, *ApJ*, 456, 305

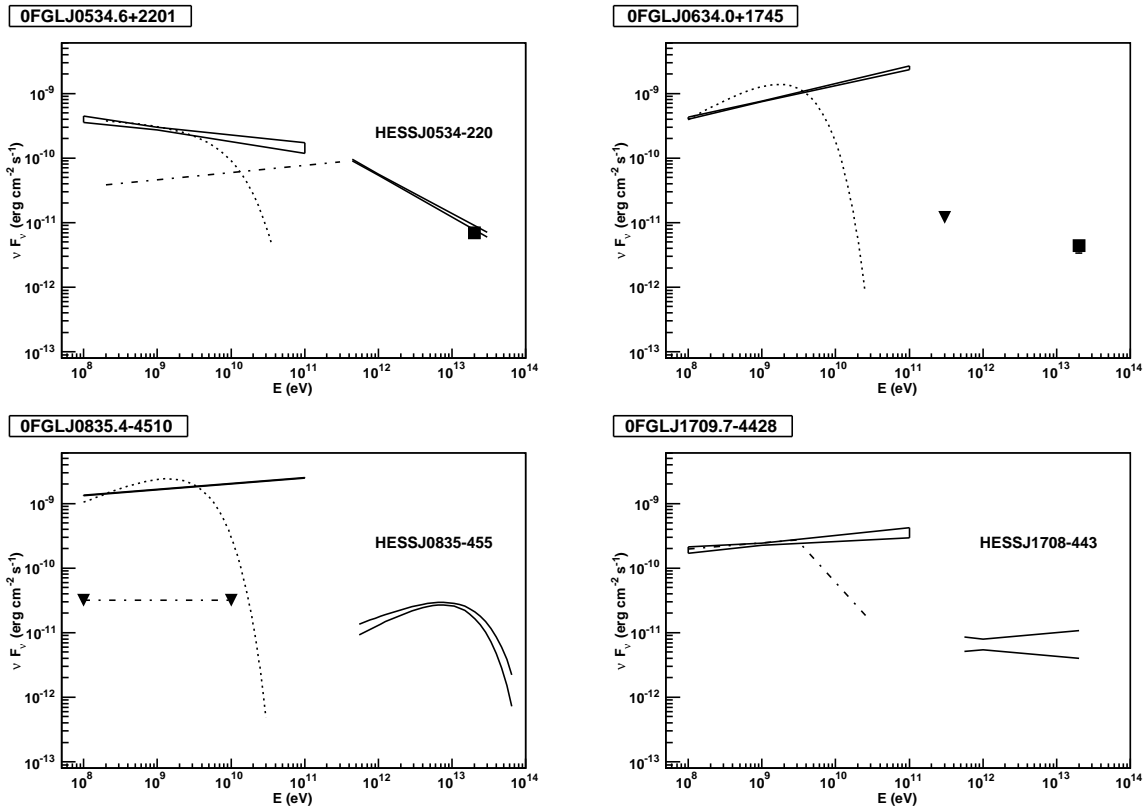


Fig. 1. MeV to TeV spectra of four EGRET pulsars and their nebula. *Upper left:* Crab (0FGL J0534.6+2201). The pulsar (dotted line) and nebula (dashed-dotted line) spectral components are those reported in Grondin et al. (2009). The VHE spectra are taken from Aharonian et al. (2006d), and the MILAGRO measurement at 20 TeV is shown (Abdo et al., 2007). *Upper right:* Geminga (0FGL J0634.0+1745). The pulsar spectrum (dotted line) are that reported in Celik et al. (2009). The triangle denotes the upper limit reported in Finnegan et al. (2009), and the MILAGRO measurement at 20 TeV is also indicated (Abdo et al., 2007). *Lower left:* Vela (0FGL J0835.4–4510). The dotted line represents the Vela spectrum as shown in Abdo et al. (2009c), while the nebula component is constrained by the two triangles joined by the dashed-dotted line. The curved VHE spectrum is taken from Aharonian et al. (2006b). *Lower right:* PSR B1706–44 (0FGL J1709.7–4428). The dashed-dotted line denotes the two power-law model spectrum derived in Gargano et al. (2009). Both LAT energy spectra (though different above 3 GeV) are consistent with the photon flux in the 1–100 GeV band of this source Abdo et al. (2009a). The VHE spectrum is taken from Hoppe et al. (2009).

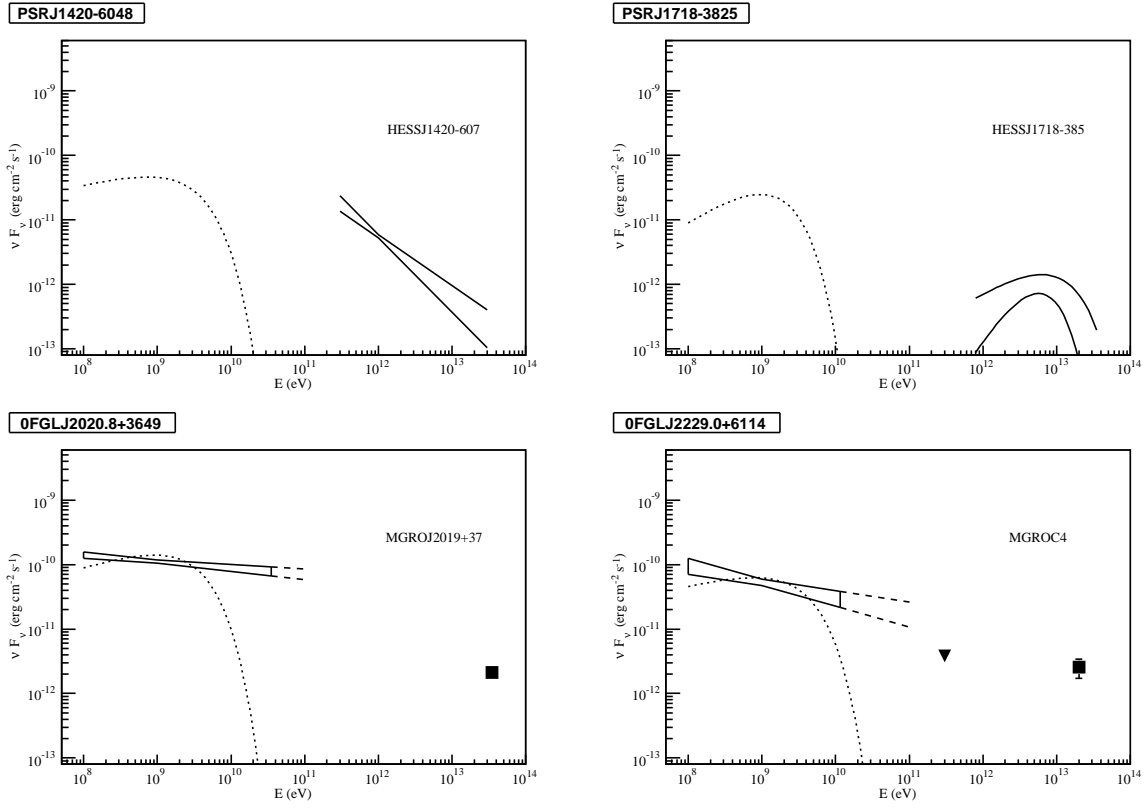


Fig. 2. MeV to TeV spectra of LAT detected pulsars that are coincident with a VHE or Milagro source. The spectra below 300 GeV are taken from Abdo et al. (2009h). *Upper left:* The VHE spectrum is taken from Aharonian et al. (2006g). *Upper right:* The VHE spectrum presented in Aharonian et al. (2007b) is shown. The two curves represent the upper and lower limits of the spectrum, taking measurement's errors into account. *Lower left:* The flux at 35 TeV is taken from Abdo et al. (2009g). *Lower right:* The flux at 20 TeV is taken from Abdo et al. (2007) and the upper limit at 300 GeV for both the pulsar and its nebula (Boomerang) is taken from de los Reyes et al. (2009).

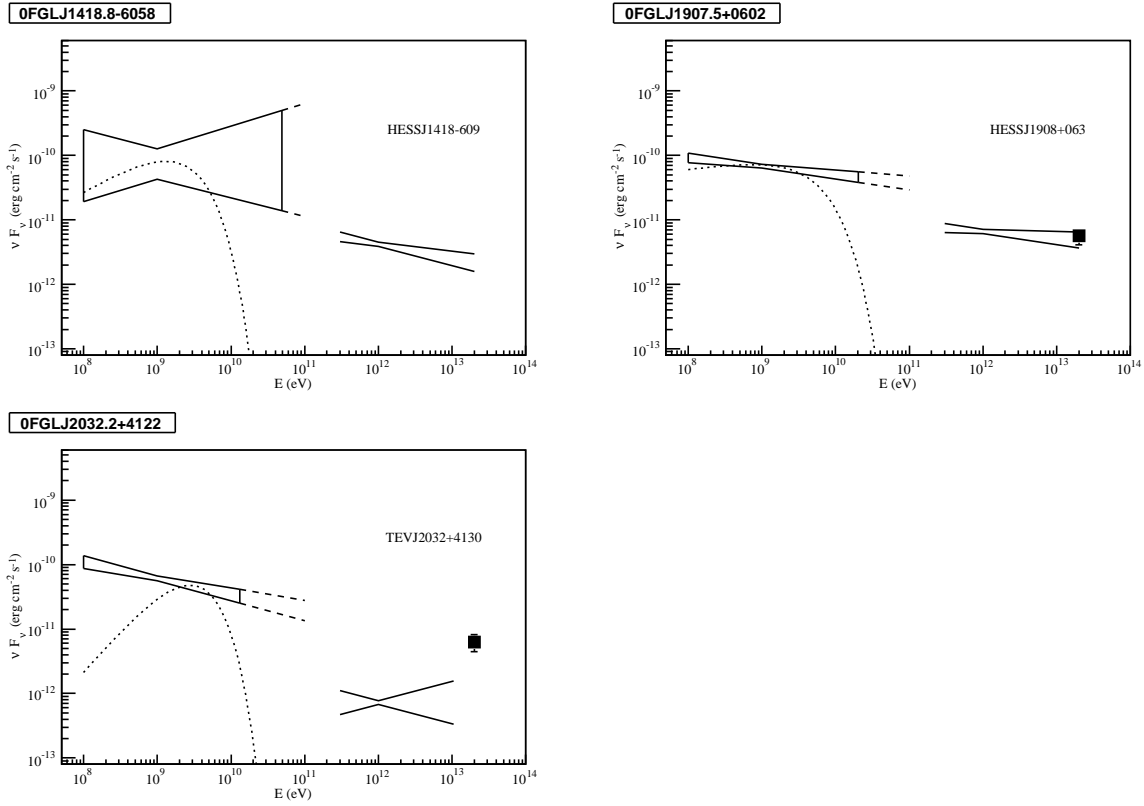


Fig. 3. MeV to TeV spectra of pulsars discovered using LAT that are coincident with a VHE source. The spectra below 300 GeV are taken from Abdo et al. (2009h). *Upper left:* The VHE spectrum is taken from Aharonian et al. (2006g). *Upper right:* The VHE spectrum presented in Djannati-Atai et al. (2008a) is shown, together with the coincident MILAGRO source flux at 20 TeV (Abdo et al., 2007). *Lower left:* The VHE spectrum is that presented in Aharonian et al. (2005b), while the MILAGRO flux at 20 TeV is also shown (Abdo et al., 2007).

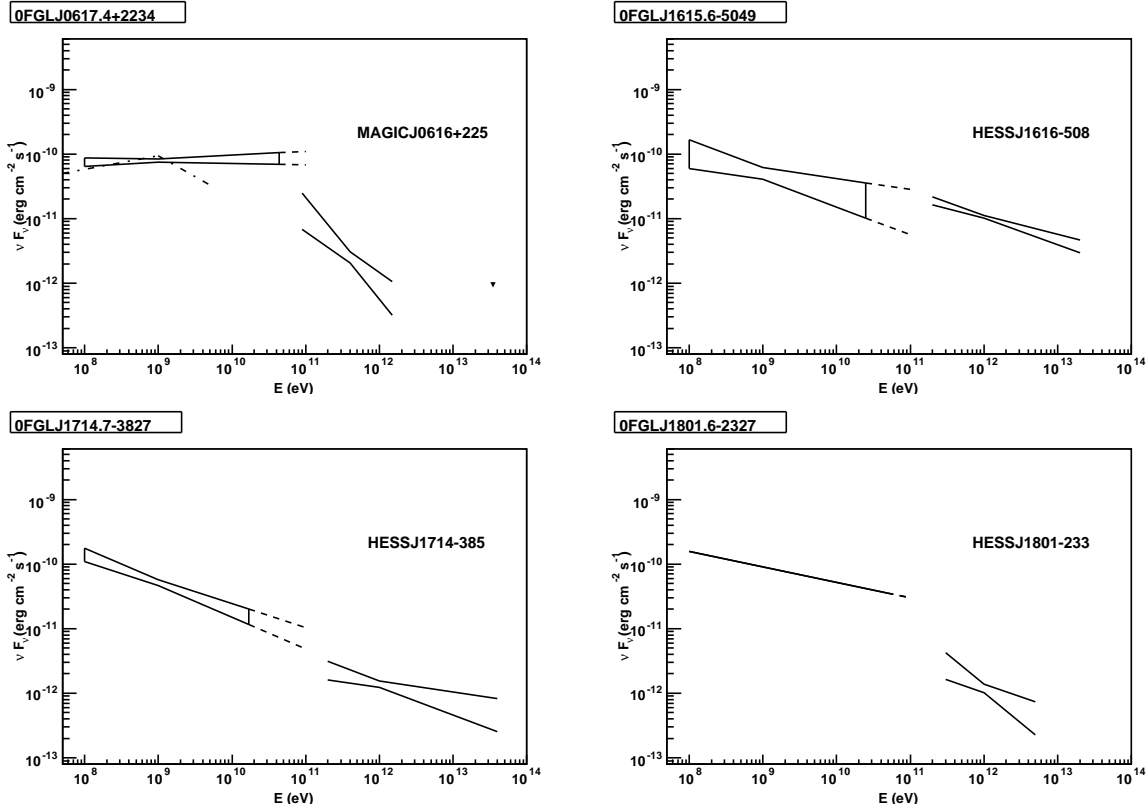


Fig. 4. MeV to TeV spectra of four SNR/PWN candidate 0FGL sources. Spectra at >100 GeV energies are taken from Albert et al. (2007) (MAGIC J0616+225), Aharonian et al. (2006f) (HESS J1616–508), Aharonian et al. (2008b) (HESS J1714–385), and Aharonian et al. (2008c) (HESS J1801–233). The broken power-law spectrum (dashed-dotted line) derived for 3EG J0617+2238 is taken from Bertsch et al. (2000). The flux at 35 TeV at the position of 0FGL J0617.4+2234 is that given in Abdo et al. (2009g).

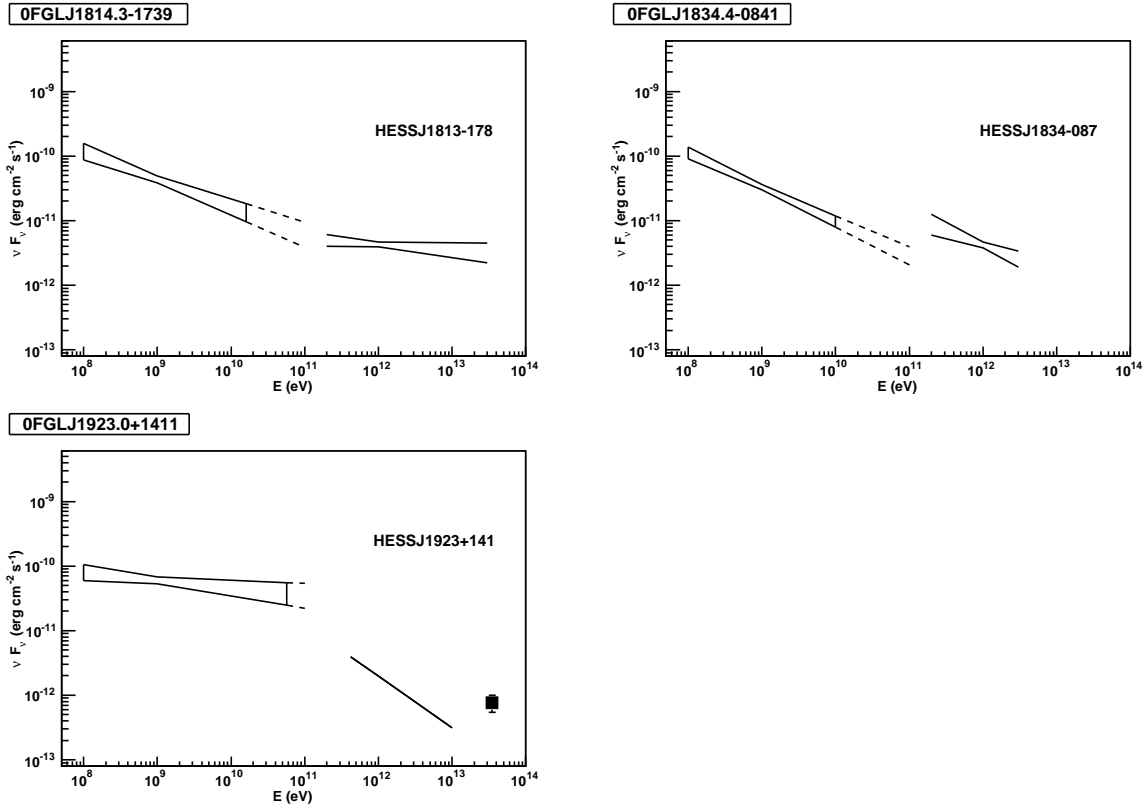


Fig. 5. MeV to TeV spectra of three SNR/PWN candidate OFGL sources. Spectra at >100 GeV energies are taken from Aharonian et al. (2006f) (HESS J1813–178 and HESS J1834–087). For HESS J1923+141, an assumed photon index of 2.8 is used in deriving the spectrum using the flux given in Fiasson et al. (2009), and the flux at 35 TeV is that given in Abdo et al. (2009g). There is evidence of a steepening above several GeV (Abdo et al., 2009e).

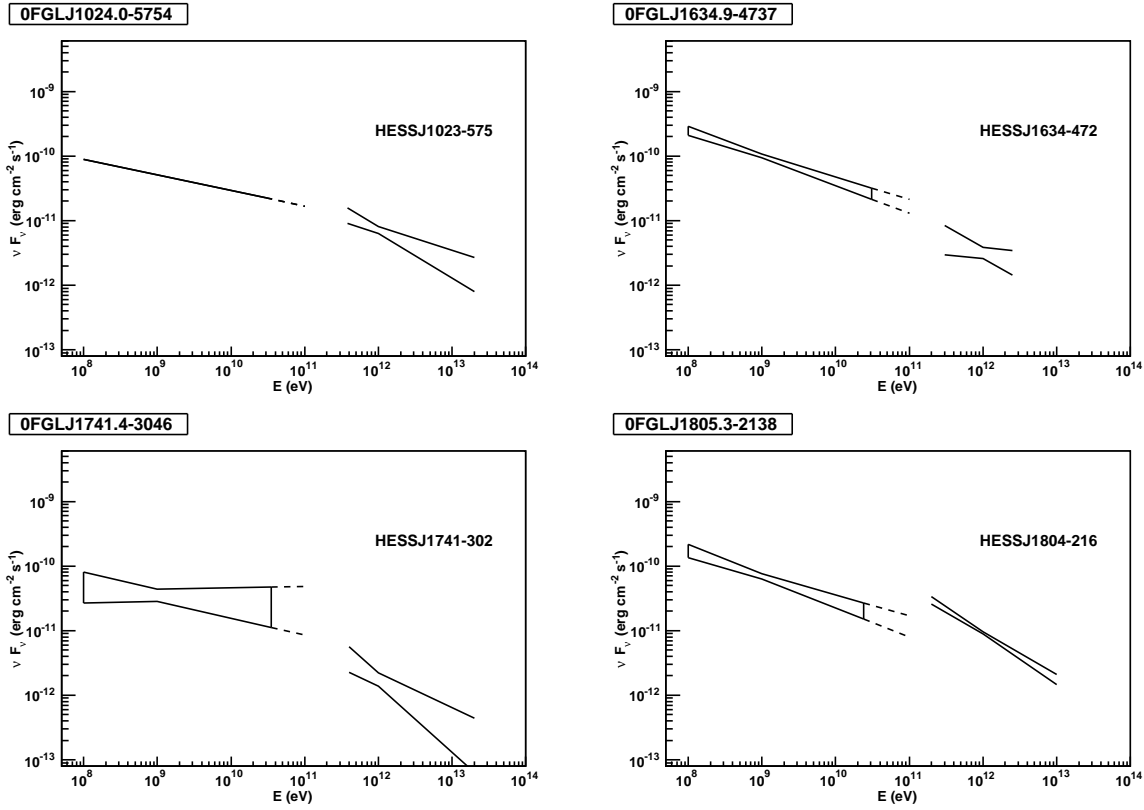


Fig. 6. MeV to TeV spectra of four unidentified 0FGL sources. Spectra at >100 GeV energies are taken from Aharonian et al. (2007a) (HESS J1023–575), Aharonian et al. (2006f) (HESS J1634–472 and HESS J1804–216), and Tibolla et al. (2009b) (HESS J1741–302).

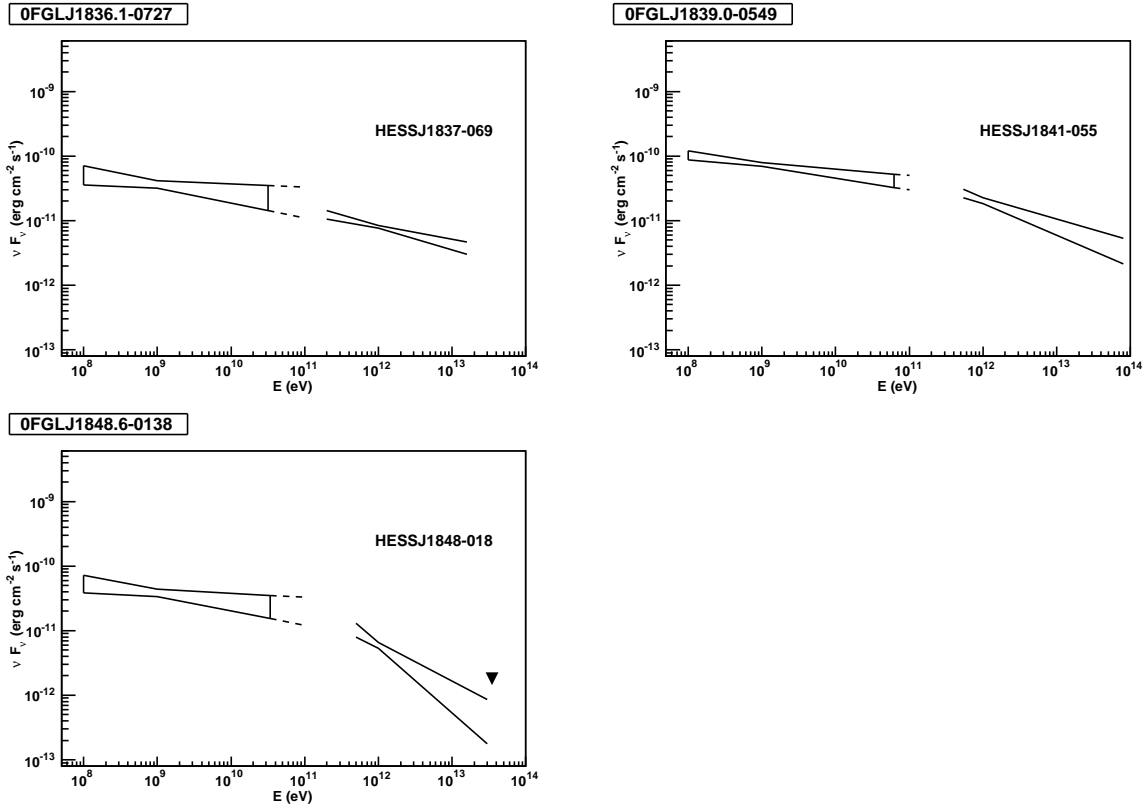


Fig. 7. MeV to TeV spectra of three unidentified 0FGL sources. Spectra at >100 GeV energies are taken from Aharonian et al. (2006f) (HESS J1837–069), Aharonian et al. (2008d) (HESS J1841–055), and Chaves et al. (2009c) (HESS J1848–018). The flux at 35 TeV at the position of 0FGL J1848.6–0138 is that given in Abdo et al. (2009g).

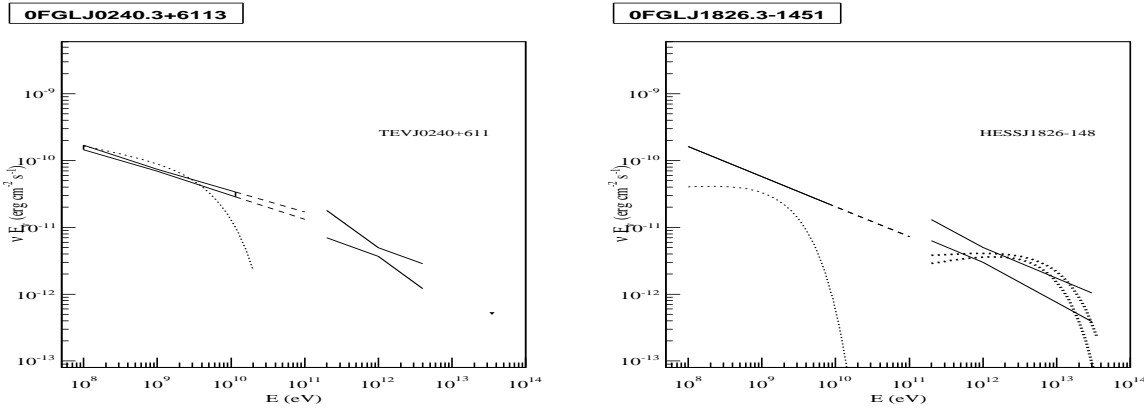


Fig. 8. MeV to TeV spectra of the two X-ray binaries in the 0FGL catalogue. The phase-averaged exponential cut-off spectrum in the GeV range of LS I +61 303 (left) is taken from Abdo et al. (2009d). That of LS 5039 is taken from Abdo et al. (2009f). Spectra at >100 GeV energies are taken from Albert et al. (2009) (for a partial phase of LS I +61 303 during which VHE emission is detected) and Aharonian et al. (2006e) (for two phases of LS 5039). The flux at 35 TeV for LS I +61 303 is that given in Abdo et al. (2009g).

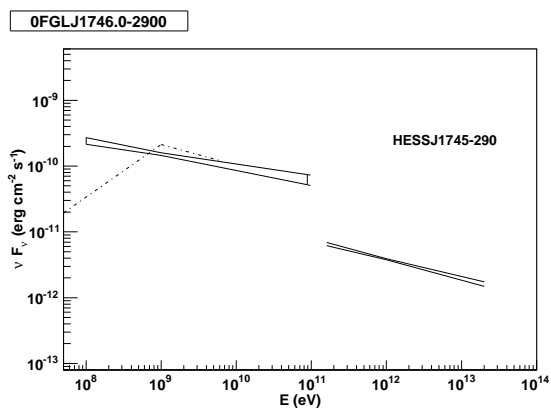


Fig. 9. MeV to TeV spectrum of the Galactic Centre. The VHE spectrum is taken from Aharonian et al. (2006h) while the broken power-law spectrum (dashed-dotted line) derived for 3EG J1746–2851 is taken from Bertsch et al. (2000).

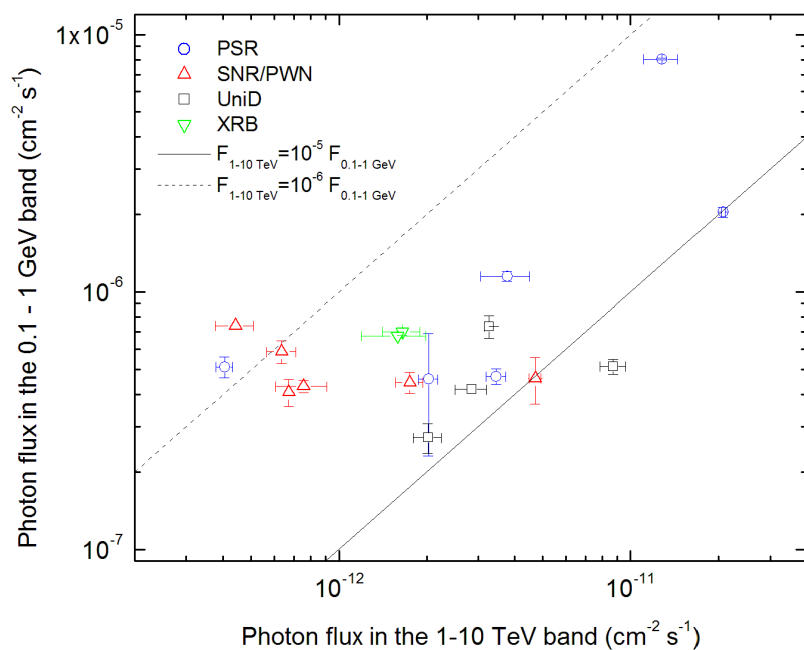


Fig. 10. Photon flux in the 100 MeV – 1 GeV band versus that in the 1–10 TeV band for coincident GeV/TeV sources

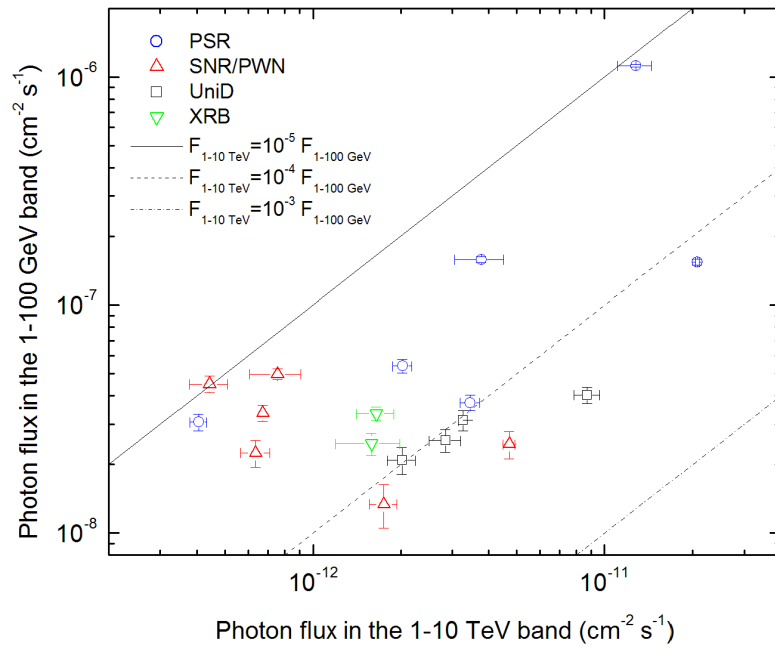


Fig. 11. Photon flux in the 1–100 GeV band versus that in the 1–10 TeV band for coincident GeV/TeV sources

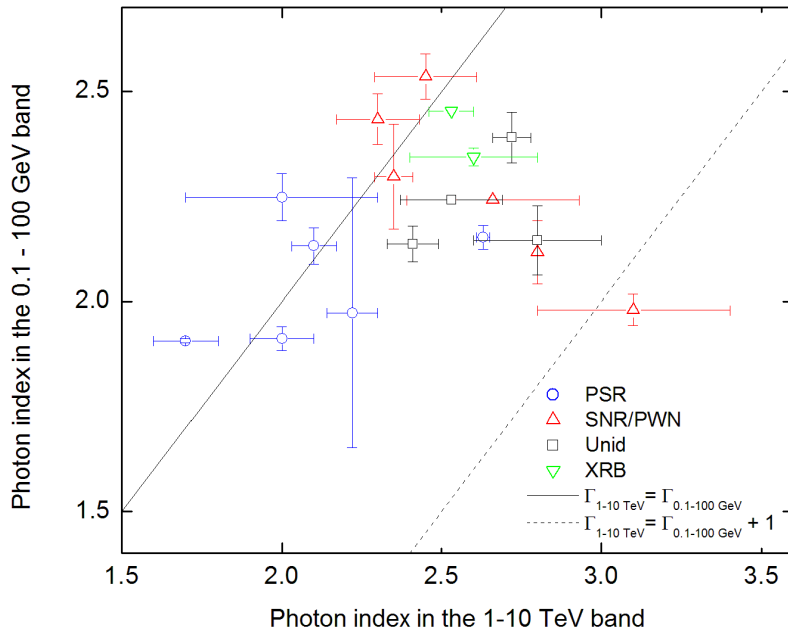


Fig. 12. Photon index in the 0.1–100 GeV band derived according to Sect. 3.1 versus photon index in the 1–10 TeV band, for coincident GeV/TeV sources. 0FGL J1923.0+1411/HESS J1923+141 is not included since its VHE photon index is not known.

Table 1. 0FGL sources with spatially coincident VHE counterpart

LAT source	association ^a	class ^b	<i>l</i> (°)	<i>b</i> (°)	error ^c (°)	VHE source	association ^d	<i>l</i> (°)	<i>b</i> (°)	ext. ^e (°)	reference
0FGL J0534.6+2201	Crab	PSR	184.56	-5.76	0.05	HESS J0534+220	Crab nebula	184.56	-5.78	PS	Aharonian et al. (2006d)
0FGL J0835.4-4510	Vela	PSR	263.56	-2.77	0.04	HESS J0835-455	Vela X	263.86	-3.09	0.43	Aharonian et al. (2006b)
0FGL J1418.8-6058		PSR	313.34	0.11	0.07	HESS J1418-609	G313.3+0.1 (Rabbit)	313.25	0.15	0.06	Aharonian et al. (2006g)
PSR J1420-6048		PSR	313.5	0.2	PS	HESS J1420-607	PSR J1420-6048	313.56	0.27	0.07	Aharonian et al. (2006g)
0FGL J1709.7-4428	PSR B1706-44	PSR	343.11	-2.68	0.05	HESS J1708-443		343.04	-2.38	0.29	Hoppe et al. (2009)
PSR J1718-3825		PSR	349.0	-0.4	PS	HESS J1718-385	G313.3+0.1 (Rabbit)	348.83	-0.49	0.015	Aharonian et al. (2007b)
0FGL J1907.5+0602		PSR	40.14	-0.82	0.08	HESS J1908+063		40.39	-0.79	0.34	Aharonian et al. (2009)
0FGL J2032.2+4122		PSR	80.16	0.98	0.09	TeV J2032+4130		80.23	1.10	0.10	Aharonian et al. (2005b)
0FGL J0617.4+2234		SNR/PWN	189.08	3.07	0.06	VER J0616.9+2230	IC 443	189.08	2.92	0.16	Acciari et al. (2009b)
0FGL J1615.6-5049		SNR/PWN	332.35	-0.01	0.23	HESS J1616-508	PSR J1617-5055?	332.39	-0.14	0.14	Aharonian et al. (2006f)
0FGL J1648.1-4606		SNR/PWN	339.47	-0.71	0.18	Westerlund 1 region		339.55 ^f	-0.40	~0.9	Ohm et al. (2009)
0FGL J1714.7-3827		SNR/PWN	348.53	0.1	0.13	HESS J1714-385	CTB 37A	348.39	0.11	0.07	Aharonian et al. (2008b)
0FGL J1801.6-2327		SNR/PWN	6.54	-0.31	0.11	HESS J1801-233	W 28	6.66	-0.27	0.17	Aharonian et al. (2008c)
0FGL J1834.4-0841		SNR/PWN	23.27	-0.22	0.1	HESS J1834-087	W 41	23.24	-0.32	0.09	Aharonian et al. (2006f)
0FGL J1923.0+1411	W 51C ^g	SNR	49.13	-0.4	0.08	HESS J1923+141	W 51	49.14	-0.6	~0.15	Fiasson et al. (2009)
0FGL J1024.0-5754		Unid	284.35	-0.45	0.11	HESS J1023-575		284.19	-0.39	0.18	Aharonian et al. (2007a)
0FGL J1805.3-2138		Unid	8.54	-0.17	0.19	HESS J1804-216	W 30/PSR J1803-2137?	8.40	-0.03	0.20	Aharonian et al. (2006f)
0FGL J1839.0-0549		Unid	26.34	0.08	0.12	HESS J1841-055		26.8	-0.2	0.42	Aharonian et al. (2008d)
0FGL J1844.1-0335		Unid	28.91	-0.02	0.15	HESS J1843-033		~29.08	~0.16	~0.2 ^h	Hoppe et al. (2008)
0FGL J1848.6-0138		Unid	31.15	-0.12	0.16	HESS J1848-018		30.98	-0.16	0.32	Chaves et al. (2009c)
0FGL J0240.3+6113	LS I +61 303	HMXB	135.66	1.08	0.07	VER J0240+612	LS I +61 303	135.70	1.08	PS	Acciari et al. (2009a)
0FGL J1826.3-1451	LS 5039	HMXB	16.89	-1.32	0.11	HESS J1826-148	LS 5039	16.90	-1.28	PS	Aharonian et al. (2006e)

^a based on timing information

^b Source class according to Abdo et al. (2009a). PSR: pulsar; SNR/PWN: supernova remnant/pulsar wind nebula; HMXB: high-mass X-ray binary; Unid: unidentified sources. The categorization of those sources as SNR/PWN is based on spatial coincidence only.

^c 95% positional error

^d based on spatial coincidence only

^e Extension. An entry of “PS” indicates that the source is point-like with respect to the point spread function of the respective instrument.

^f The VHE emission has been detected using H.E.S.S. towards the direction of the massive stellar cluster. The coordinates refer to the nominal position of Westerlund 1

^g The association is based on a morphological study (Abdo et al., 2009e).

^h The extent of the source is not clear. The given value is estimated from the sky excess map in the corresponding reference.

Table 2. 0FGL sources with coincident MILAGRO source, but without plausible coincident reported VHE sources. See Table 1 for the nomenclature.

LAT source	Class	<i>l</i> (°)	<i>b</i> (°)	error (°)	Milagro source (°)	<i>l</i> (°)	<i>b</i>	reference
0FGL J0634.0+1745	PSR	195.16	4.29	0.04	MGRO C3	195.7	4.1	Abdo et al. (2007)
0FGL J2020.8+3649	PSR	75.182	0.131	0.060	MGRO J2019+37	75.0	0.2	Abdo et al. (2007)
0FGL J2229.0+6114	PSR	106.644	2.956	0.08	MGRO C4	105.8	2.0	Abdo et al. (2007)

Table 3. OFGL sources with possibly coincident VHE source. See Table 1 for the nomenclature.

LAT source	class	l ($^{\circ}$)	b ($^{\circ}$)	error ($^{\circ}$)	VHE source	association	l ($^{\circ}$)	b ($^{\circ}$)	ext. ($^{\circ}$)	reference
OFGL J1814.3–1739	SNR/PWN	13.05	-0.09	0.19	HESS J1813–178	G12.8–0.2/AX J1813–178	12.81	-0.03	0.04	Aharonian et al. (2006f)
OFGL J1634.9–4737	Unid	336.84	-0.03	0.08	HESS J1634–472		337.11	0.22	0.11	Aharonian et al. (2006f)
OFGL J1741.4–3046	Unid	357.96	-0.19	0.2	HESS J1741–302		358.4	0.01	?	Tibolla et al. (2009b)
OFGL J1746.0–2900	Unid	359.99	-0.11	0.07	HESS J1745–290	Sgr A*/G359.95–0.04	359.94	-0.04	PS	van Eldik et al. (2008)
OFGL J1836.1–0727	Unid	24.56	-0.03	0.22	HESS J1837–069		25.18	-0.12	$7^m 2 \times 3'$	Aharonian et al. (2006f)

Table 4. H.E.S.S. sources with coincident OFGL source which do not have a 3EG counterpart as in Reimer et al. (2008)

H.E.S.S. sources	OFGL sources	coincidence level
HESS J1616–508	OFGL J1615.6–5049	Y
HESS J1634–472	OFGL J1634.9–4737	P
HESS J1745–290	OFGL J1746.0–2900	P
HESS J1804–216	OFGL J1805.3–2138	Y
HESS J1834–087	OFGL J1834.4–0841	Y
HESS J1837–069	OFGL J1836.1–0727	P

Table 5. Number of coincidence cases for each source population excluding AGN in the region $l = -85^{\circ}$ to 60° , $b = -3^{\circ}$ to 3° .

LAT Source class	OFGL sources	spatially coincident cases ^a
pulsars	10	4
SNR/PWN candidates	11	6 (7)
Unidentified sources	19	5 (9)
Total ^b	41	16 (21)

^a The numbers in brackets include slightly offset cases (P).^b including LS 5039